

Looking into the Theory of Pulsar Accretion: Cen X-3 and XTE J1946+274

Diana M. Marcu^{*†}

Department of Physics & Center for Space Science and Technology, UMBC, Baltimore, MD 21250, USA

CRESST & NASA Goddard Space Flight Center, Greenbelt, MD 20771, USA

E-mail: diana.m.marcu@nasa.gov

Katja Pottschmidt

Department of Physics & Center for Space Science and Technology, UMBC, Baltimore, MD 21250, USA

CRESST & NASA Goddard Space Flight Center, Greenbelt, MD 20771, USA

E-mail: katja@milkyway.gsfc.nasa.gov

Amy Gottlieb

Department of Physics & Center for Space Science and Technology, UMBC, Baltimore, MD 21250, USA

CRESST & NASA Goddard Space Flight Center, Greenbelt, MD 20771, USA

E-mail: amygl@umbc.edu

Michael T. Wolff

Center for Space Research, Naval Research Laboratory, Washington DC , 20375 USA

E-mail: Michael.Wolff@nrl.navy.mil

Peter A. Becker

Center for Earth Observing and Space Research, George Mason University, Fairfax, VA 22030-4444, USA

E-mail: pbecker@gmu.edu

Jörn Wilms

Remeis-Observatory & ECAP, Universität Erlangen-Nürnberg, 96049 Bamberg, Germany

E-mail: joern.wilms@sternwarte.uni-erlangen.de

Carlo Ferrigno

ISDC, Department of Astronomy, Université de Genève, chemin d'Écogia, 16, CH-1290 Versoix, Switzerland

E-mail: Carlo.Ferrigno@unige.ch

Kent S. Wood

Center for Space Research, Naval Research Laboratory, Washington DC , 20375 USA

E-mail: Kent.Wood@nrl.navy.mil

This is an overview of pulsar accretion modeling. The physics of pulsar accretion, i.e., the process of plasma flow onto the neutron star surface, can be constrained from the spectral properties of the X-ray source. We discuss a new implementation of the physical continuum model developed by Becker and Wolff (2007, ApJ 654, 435). The model incorporates Comptonized blackbody, bremsstrahlung, and cyclotron emission. We discuss preliminary results of applying the new tool to the test cases of *Suzaku* data of Cen X-3 and XTE J1946+274. Cen X-3 is a persistent accreting pulsar with an O-star companion observed during a bright period. XTE J1946+274 is a transient accreting pulsar with a Be companion observed during a dim period. Both sources show spectra that are well described with an empirical Fermi Dirac cutoff power law model. We extend the spectral analysis by making the first steps towards a physical description of Cen X-3 and XTE J1946+274.

10th INTEGRAL Workshop: A Synergistic View of the High-Energy Sky
15-19 September 2014
Annapolis, MD, USA

*Speaker.

†On behalf of the Magnet Collaboration

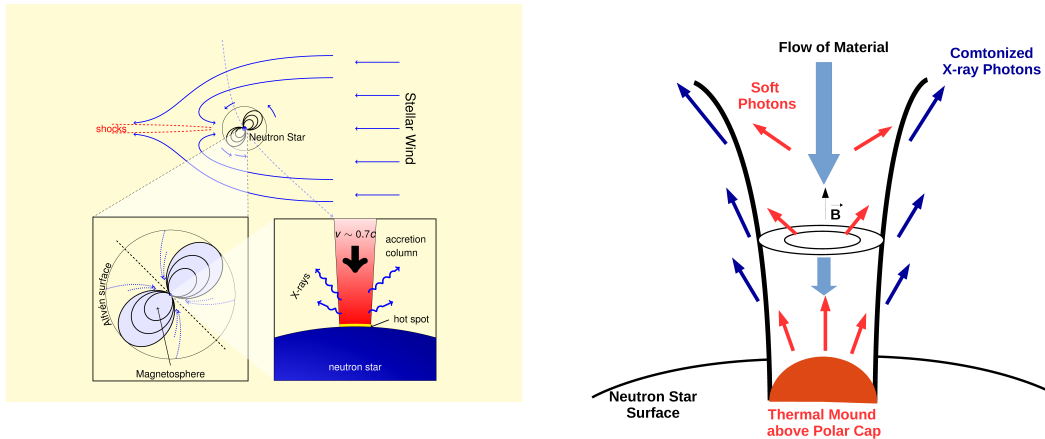


Figure 1 **Left:** Schematic representation of accretion from a wind-emitting star onto a magnetized neutron star. After Davidson & Ostriker (1973). **Right:** Illustration of plasma flowing through the accretion column onto the magnetic pole of a neutron star. The soft photons are created through blackbody, bremsstrahlung and cyclotron emission. After Becker & Wolff (2007).

1. Introduction

X-ray pulsars are binary systems in which material from the donor star is accreted onto a neutron star with a strong magnetic field. The first physical continuum model for accreting pulsars was provided by two of the coauthors, i.e., the Becker and Wolff 2007 (B&W) model Becker & Wolff (2007). The left panel in Figure 1 illustrates how as the material approaches the star, it couples with the magnetic field lines at the Alfvén radius. As the material falls towards the surface of the neutron star, it decelerates and produces bremsstrahlung emission. Cyclotron emission is also present due to the pulsar’s strong magnetic field. Finally, as the material settles on the surface of the neutron star, it forms a thermal mound which emits blackbody radiation. The B&W model is a bulk and thermal Comptonization model which incorporates the three types of seed photons (blackbody, bremsstrahlung, and cyclotron) that are then Comptonized into the approximate power law spectrum that we see in accreting pulsars, see right panel in Figure 1. We are working on implementing this model for statistical fitting, e.g. in `xspec` or `isis`, and making it publicly available. Currently phenomenological models are generally used to describe the cutoff power law continuum shape of accreting pulsars.

2. Observations

We will first introduce the sources, Cen X-3 and XTE J1946+274, and discuss empirical modeling of their *Suzaku* spectra. We will then present the first results of applying the B&W model to these spectra.

2.1 Centaurus X-3

Cen X-3 was the first X-ray pulsar discovered in a 1971 observation, with *Uhuru* Giacconi et al.

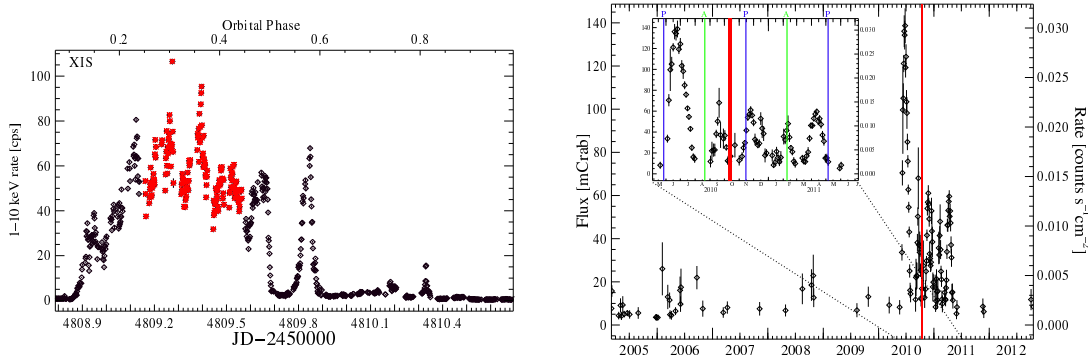


Figure 2 **Left** - *Suzaku*-XIS lightcurve of an observation of a full Cen X-3 orbit in 2008, December. The spectral analysis was performed on the data highlighted in red (after Gottlieb et al., in prep.). **Right** - *Swift*-BAT lightcurve of XTE J1946+274 with the time of the *Suzaku* observation marked as the red vertical line. The upper-left panel shows a closer view of the 2010 series of outbursts with apastron and periastron times (after Marcu et al., in prep.).

(1971). Cen X-3 is a persistent High Mass X-ray Binary (HMXB) composed of a neutron star with a mass of $1.21 \pm 0.21 M_{\odot}$ and a pulse period of ~ 4.8 s which orbits an O6.5II-type companion with a mass of $20.5 \pm 0.7 M_{\odot}$ Ash et al. (1999). The X-ray source is eclipsed $\sim 20\%$ of its 2.1 d orbit. Cen X-3 also exhibits several spectral features: three iron (Fe) fluorescent lines at 6.4 keV, 6.7 keV and 6.9 keV Naik et al. (2011), a Cyclotron Scattering Resonance Feature (CRSF) at ~ 30 keV Suchy et al. (2008), and a broad “10 keV bump” at ~ 13 keV, a feature which is relatively common in accreting pulsars Coburn et al. (2002); Mihara (1995).

We studied a 90 ks *Suzaku* observation spread out over a full orbital period observed in 2008, December 8 – 10, eclipse to eclipse, as can be seen in the left panel of Figure 2. The spectra shown in the left panel of Figure 3 were extracted from a bright part of the lightcurve (shown in red in the left panel of Figure 2) in which the hardness ratio was approximately constant. Considering a distance to the source of ~ 8 kpc Krzeminski (1974), the 1 – 40 keV luminosity for the extracted bright part is $\sim 1.2 \times 10^{38}$ erg/s.

We modeled the XIS and PIN spectra (Gottlieb et al., in prep.) by taking into account the following components in *xspec*: the cross-normalization between the instruments modeled with a constant, the partial covering absorption modeled with *tbnew_pcf* and *tbnew_feo*¹ Wilms et al. (2000), the three Fe emission lines modeled with Gaussian lines (*gauss*), the 13 keV feature modeled with another Gaussian line, and a CRSF at ~ 30 keV modeled with a Gaussian optical depth profile (*gabs*)². The continuum was best fitted with a Fermi Dirac cutoff model Tanaka (1986) described by:

$$M_{\text{fdecut}}(E) \propto E^{-\Gamma} \times \left[1 + \exp\left(\frac{E - E_{\text{cut}}}{E_{\text{fold}}}\right) \right]^{-1}. \quad (2.1)$$

At energy E the photon flux is described by a power law with a photon index Γ , multiplied by an

¹Tbnew is an updated version of tbabs, see <http://pulsar.sternwarte.uni-erlangen.de/wilms/research/tbabs/> for more details.

²Three additional Gaussian lines were included to model weak residuals. They will be discussed in Gottlieb et al., in prep.

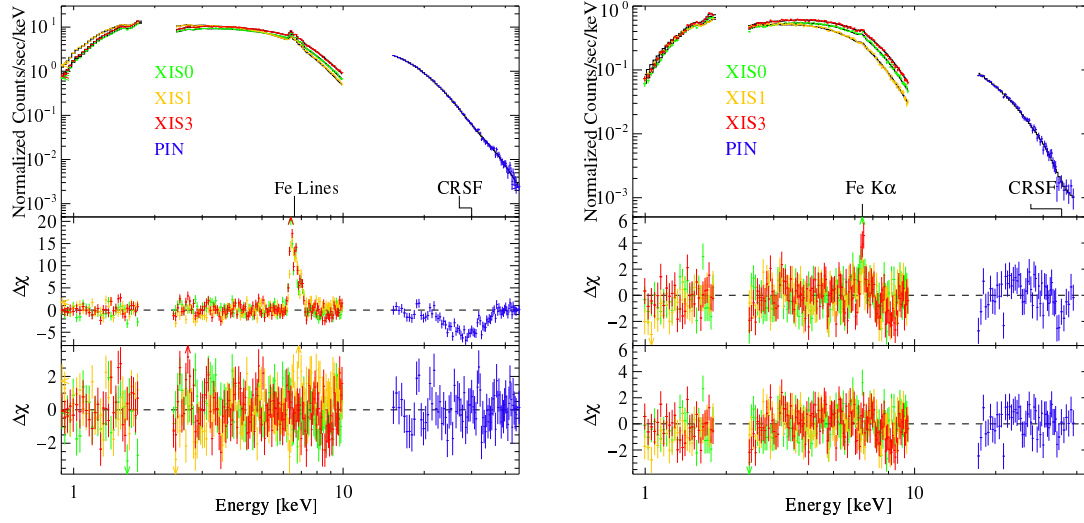


Figure 3 Top: *Suzaku* spectra of the Cen X-3 data highlighted in red in the left panel of Figure 2 (left) and *Suzaku* spectra of XTE J1946+274 (right) with the Fermi Dirac cutoff power law best fit model (black line). Middle: Residuals of the fitted absorbed continuum without the Fe line and CRSF. Bottom: Residuals after including the Fe Gaussian line and CRSF. Selected best fit parameters are listed in Table 1.

exponential cutoff at energy E_{cut} with a folding energy E_{fold} . The final best fit model is:

$$M_{\text{Cen X-3}}(E) = \text{const} \times \text{tbnew_pcf} \times \text{tbnew_feo} \times (\text{power} \times \text{fdcut} + 3 \times \text{gauss}_{\text{Fe}} + \text{gauss}_{10\text{keV}} + 3 \times \text{gauss}_{\text{weak}}) \times \text{gabs}_{\text{CRSF}}. \quad (2.2)$$

Selected parameters of this empirical fit are listed in Table 1. The continuum parameters are highlighted. Those are the standard model parameters that describe the continuum which we are trying to describe with the physical B&W model.

Applying an analytical test implementation of the full B&W model (in Fortran), we performed a fit “by eye” to the **unfolded, unabsorbed** *Suzaku* data of Cen X-3. The result is shown in the left panel of Figure 4 with the physical parameters listed in Table 2. The results are promising since the model qualitatively agrees with the data. The emission is bremsstrahlung dominated overall, with a strong contribution from cyclotron emission. The CRSF is not implemented in the model and, therefore, we can see the model overpredicting the flux around 30 keV where the observed spectrum shows a broad dip due to the magnetic resonant scattering of the photons. The Fe fluorescent lines, which are also not part of the continuum model, can be seen in the 6-7 keV region.

2.2 XTE J1946+274

XTE J1946+274 was discovered in 1998 September by the All-Sky Monitor (ASM), on board of the Rossi X-ray Timing Explorer (*RXTE*) Smith & Takeshima (1998). In contrast to the bright and persistent Cen X-3, XTE J1946+274 is a transient HMXB which has shown only two series of outbursts: three months in 1998 at discovery and several months in 2010-2011. The optical companion is a giant Be-IV-IVe star Verrecchia et al. (2002) orbited by a ~ 15.7 s pulsar Müller

et al. (2012). The orbital period is ~ 169.2 d, the orbital inclination is $\sim 46^\circ$ and the distance to the source is 9.5 ± 2.9 kpc Wilson et al. (2003). The source shows ~ 2 outbursts per orbit, an unusual behavior for Be systems in which only one outburst per orbit is generally observed. During the 1998 series a CRSF was detected at ~ 35 keV Heindl et al. (2001). XTE J1946+274 also shows an Fe fluorescent line at 6.4 keV.

We extracted *Suzaku* XIS and PIN spectra from a 42 ks observation taken on 2010 October 12, during a minimum between two outburst from the 2010 series (see right panel of Figure 2). During the observation the source had a 1 – 40 keV luminosity of $\sim 3.4 \times 10^{36}$ erg/s (much lower than that of Cen X-3). Similarly to Cen X-3, we modeled the XIS and PIN data (Marcu et al., in prep.) taking into consideration the instrument cross calibration, absorption, a Gaussian Fe line, and a weak CRSF line. Even though these sources have very different characteristics (e.g. luminosity, optical companion, frequency of bright periods, orbital periods, etc.) their continua are well described with the same empirical model, `fdcut`³. The best fit model for XTE J1946+274 in `xspec` notation is:

$$M_{\text{XTE J1946+274}}(E) = \text{const} \times \text{tbnew_feo} \times (\text{power} \times \text{fdcut} + \text{gauss}_{\text{Fe}}) \times \text{gabs}_{\text{CRSF}}. \quad (2.3)$$

Selected parameters for this fit are listed in Table 1. The continuum parameters for XTE J1946+274 are also highlighted.

Similarly to Cen X-3, we performed a “fit by eye” to the unfolded, unabsorbed *Suzaku* data of XTE J1946+274 using the new B&W model implementation. As can be seen in the right panel in Figure 4, the continuum is again dominated by bremsstrahlung emission, but with a much weaker contribution from cyclotron line emission than we found in Cen X-3. The model again agrees well with the data, particularly at lower energies. The physical model parameters applied towards this “fit” are listed in Table 2. As expected, due to the difference in luminosity between the two sources, the mass accretion rate, electron temperature inside the column, as well as the radius of the accretion column are lower for XTE J1946+274 than they are for the high-luminosity source Cen X-3.

3. Current and Future Applications

An earlier application of the B&W model was carried out for the source 4U 0115+63 using broad-band *BeppoSAX* data accumulated during an outburst decay, see Ferrigno et al. (2009) and `xspec` model available from C. Ferrigno. In this case the emission from the column is dominated by Compton scattered cyclotron emission because of the relatively low magnetic field of this source. Its contribution is dominant above ~ 7 keV. Below this energy, it was necessary to include a thermal Comptonization component, which is interpreted as coming from a scattering halo surrounding the neutron star surface.

The “`compMag`” model Farinelli et al. (2012) provides a numerical solution of the radiative transfer equation in a cylindrical column with approximate cross sections for scattering in a magnetized plasma using similar assumptions as the B&W model. In the version available for `Xspec`,

³Note that this empirical description is not unique, see Marcu et al., in prep. for the application of all commonly used empirical models, yielding comparable fit quality.

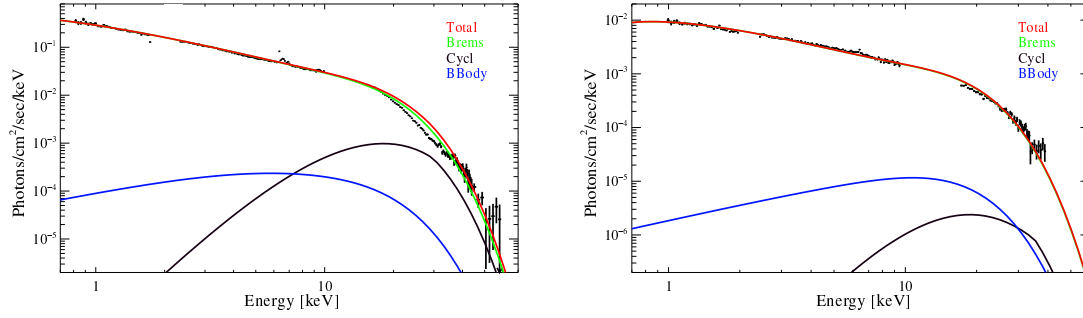


Figure 4 Fit “by eye” applying the B&W physical model to the *Suzaku* data (black) of Cen X-3 (left) and XTE J1946+274 (left). The three types of Comptonized emission are shown: bremsstrahlung in green, cyclotron emission in dark purple and back body emission in blue. The physical parameters are listed in Table 3.

only blackbody seed photons are taken into account in an exponential distribution along the accretion column. This model allows the user to switch between two different velocity profiles of the in falling plasma. Work is in progress to include emission from the magnetized optically thin plasma of the accretion stream and will be presented in a forthcoming publication, see also Ferrigno et al. (2014).

Here we presented promising first steps towards the physical modeling of accreting pulsars using a new analytical implementation of the B&W model. In order to determine the robustness of the physical parameters statistical modeling is required and we are currently implementing the analytical model into `xspec`. The analytical and numerical versions of the model will be tested on observed X-ray spectra of several accreting pulsars starting with Cen X-3, XTE J1946+274, 4U 0115+63 and GX 304–1. We plan to conduct a thorough comparison between the empirical and physical fits. This will allow us to physically interpret data of accreting pulsars previously analyzed with empirical models.

	Cen X-3	XTE J1946+274
N_{H}^a	$4.8^{+2.3}_{-1.3}$	-
f	$0.26^{+0.10}_{-0.06}$	-
N_{H}^a	$1.61^{+0.07}_{-0.05}$	$1.67(3)$
A_{Γ}^b	$0.37^{+0.09}_{-0.03}$	$2.05^{+0.04}_{-0.05}{}^c$
Γ	$1.06^{+0.16}_{-0.05}$	$0.57(2)$
$E_{\text{cut}} [\text{keV}]$	$17.7^{+2.7}_{-3.3}$	$0.05^{+0.03}_{-0.05}{}^c$
$E_{\text{fold}} [\text{keV}]$	$7.0^{+0.07}_{-0.06}$	$8.9(4)$
$E_{\text{CRSF}} [\text{keV}]$	$30.3(9)$	$35.2^{+1.5}_{-1.3}$
$\chi^2_{\text{red}}/\text{dof}$	$1.31/500$	$1.17/466$

Table 1 Main best fit model parameters for the Fermi Dirac cutoff power law fits to the *Suzaku* spectra of Cen X-3 and XTE J1946+274. The continuum parameters are highlighted. The full list of fit parameters can be found in Gottlieb et al., in prep. for Cen X-3 and Marcu et al., in prep. for XTE J1946+274. (a) $\times 10^{22} \text{cm}^{-2}$; (b) $\text{keV}^{-1} \text{cm}^{-2} \text{s}^{-1}$; (c) $\times 10^{-2}$.

	Cen X-3	XTE J1946+274
$\dot{M} [\times 10^{17} \text{g/s}]$	11.32	1.4
$T_{\text{e}} [\times 10^7 \text{K}]$	3.74	3.4
$B [\times 10^{12} \text{G}]$	2.55	3.04
$r_0 [\text{m}]$	700	100
σ_{\parallel}^d	1.01	2.141
$\bar{\sigma}^d$	9.317	12.79

Table 2 Physical parameters used for a “fit by eye” of the B&W model for the *Suzaku* data of Cen X-3 and XTE J1946+274. The physical parameters are: mass accretion rate, \dot{M} ; electron temperature inside the column, T_{e} ; magnetic field strength in the emission line region, B ; radius of the accretion column, r_0 ; the scattering cross sections parallel to the magnetic field (σ_{\parallel}) and the average cross section ($\bar{\sigma}$) as a function of the Thompson cross section, σ_{T} . (d) $\times 10^{-4} \sigma_{\text{T}}$.

References

- Ash, T. D. C., Reynolds, A. P., Roche, P., et al. 1999, MNRAS, 307, 357
- Becker, P. A., & Wolff, M. T. 2007, Astrophys. J., 654, 435
- Coburn, W., Heindl, W. A., Rothschild, R. E., et al. 2002, Astrophys. J., 580, 394
- Davidson, K., & Ostriker, J. P. 1973, Astrophys. J., 179, 585
- Farinelli, R., Ceccobello, C., Romano, P., & Titarchuk, L. 2012, Astron. Astrophys., 538, A67
- Ferrigno, C., Becker, P. A., Segreto, A., Mineo, T., & Santangelo, A. 2009, Astron. Astrophys., 498, 825
- Ferrigno, C., Farinelli, R., & Bozzo, E. 2014, in The X-ray Universe 2014, 72
- Giacconi, R., Gursky, H., Kellogg, E., Schreier, E., & Tananbaum, H. 1971, Astrophys. J., Lett., 167, L67
- Heindl, W. A., Coburn, W., Gruber, D. E., et al. 2001, Astrophys. J., Lett., 563, L35
- Krzeminski, W., 1974, Astrophys. J., Lett., 192, L135
- Mihara, T., 1995, Ph.D. thesis, , Dept. of Physics, Univ. of Tokyo (M95)
- Müller, S., Kühnel, M., Caballero, I., et al. 2012, Astron. Astrophys., 546, A125
- Naik, S., Paul, B., & Ali, Z. 2011, Astrophys. J., 737, 79

- Smith, D. A., & Takeshima, T. 1998, *The Astronomer's Telegram*, 36, 1
- Suchy, S., Pottschmidt, K., Wilms, J., et al. 2008, *Astrophys. J.*, 675, 1487
- Tanaka, Y., 1986, in *IAU Colloq. 89: Radiation Hydrodynamics in Stars and Compact Objects*, ed. D. Mihalas, K.-H. A. Winkler, Vol. 255, *Lecture Notes in Physics*, Berlin Springer Verlag, 198
- Verrecchia, F., Israel, G. L., Negueruela, I., et al. 2002, *Astron. Astrophys.*, 393, 983
- Wilms, J., Allen, A., & McCray, R. 2000, *Astrophys. J.*, 542, 914
- Wilson, C. A., Finger, M. H., Coe, M. J., & Negueruela, I. 2003, *Astrophys. J.*, 584, 996